SAND2000-1065C

Modeling of Transient Ionizing Radiation Effects in Bipolar Devices at High Dose-Rates

T. A. Fjeldly,[1,2] Y. Deng,[2] M. S. Shur,[2] H. P. Hjalmarson,[3] and A. Muyshondt[3]

[1]UniK- Norwegian University of Science and Technology, N-2027 Kjeller, Norway
[2]ECSE Department, Rensselaer Polytechnic Institute, Troy, NY 12180-3590
[3]Sandia National Laboratories, Albuquerque, NM 87185

1. Introduction

To optimally design circuits for operation at high intensities of ionizing radiation, and to accurately predict their behavior under radiation, precise device models are needed that include both stationary and dynamic effects of such radiation. Depending on the type and intensity of the ionizing radiation, different degradation mechanisms, such as photoelectric effect, total dose effect, or single even upset might be dominant.[1] In this paper, we consider the photoelectric effect associated with the generation of electron-hole pairs in the semiconductor.

The effects of low radiation intensity on *p-n* diodes and bipolar junction transistors (BJTs) were described by low-injection theory in the classical paper by Wirth and Rogers.[2] However, in BJTs compatible with modern integrated circuit technology, high-resistivity regions are often used to enhance device performance, either as a substrate or as an epitaxial layer such as the low-doped *n*-type collector region of the device. Using low-injection theory, the transient response of epitaxial BJTs was discussed by Florian et al.[3], who mainly concentrated on the effects of the Hi-Lo (high doping - low doping) epilayer/substrate junction of the collector, and on geometrical effects of realistic devices.

For devices with highly resistive regions, the assumption of low-level injection is often inappropriate, even at moderate radiation intensities, and a more complete theory for high-injection levels was needed. In the dynamic photocurrent model by Enlow and Alexander,[4] *p-n* junctions exposed to high-intensity radiation were considered. In their work, the variation of the minority carrier lifetime with excess carrier density, and the effects of the ohmic electric field in the quasi-neutral (q-n) regions were included in a simplified manner. Later, Wunsch and Axness[5] presented a more comprehensive model for the transient radiation response of *p-n* and *p-i-n* diode geometries. A stationary model for high-level injection in *p-n* junctions was developed by Isaque et al.[6] They used a more complete ambipolar transport equation, which included the dependencies of the transport parameters (ambipolar diffusion constant, mobility, and recombination rate) on the excess minority carrier concentration. The expression used for the recombination rate was that of Shockley-Reed-Hall (SRH) recombination, which is dominant for low to mid-level radiation intensities. However, at higher intensities, Auger recombination becomes important eventually dominant.

The complete ambipolar transport equation, including the complicated dependence of transport parameters on the radiation intensity, cannot be solved analytically. We therefore find an approximate This solution is obtained for each of the regimes where a given recombination mechanism dominates, and then by joining these solutions using appropriate smoothing functions. This approach allows us to develop a BJT model accounting for the photoelectric effect of the ionizing radiation that can be implemented in SPICE.

2. SPICE Model

In circuit simulators such as SPICE, the device models are defined in terms of equivalent circuits consisting of circuit elements such as current sources, capacitances, resistances, etc. Adding suitable equivalent circuits for the photoelectric effect, such models implemented in SPICE can be used for simulating the dynamic behavior of irradiated devices. In the present models, we represent the stationary and dynamic photocurrents by using a current source in parallel with each *p-n*-junction, as shown in Fig. 1 for the basic Gummel-Poon BJT model.[7,8,9] These current sources include the prompt photocurrent associated with the generation of electron-hole (e-h) pairs in the depletion regions, and the delayed response associated with the build-up and discharge of excess charge carriers in the q-n regions adjacent to the junctions. The latter are described in terms of a characteristic delay time for each q-n region, which can be represented by RC equivalent delay circuits, as shown to the right in Fig. 1. However, since the delay times are determined by the ambipolar transport parameters within the q-n regions, they will be dynamic quantities determined by the momentary minority carrier charge. The momentary conditions are described in terms of dynamic "generation rates" G_n and G_p associated with each q-n region.

2.1. Stationary model

The photocurrent in a diode structure consists of three terms: the drift term for electron-hole pairs produced in the diode depletion region, and the ambipolar transport of charge carrier in the two q-n regions adjacent to the

DISCLAIMER

DISCLAIMER

Portions of this document may be illegible in electronic image products. Images are produced from the best available original document.

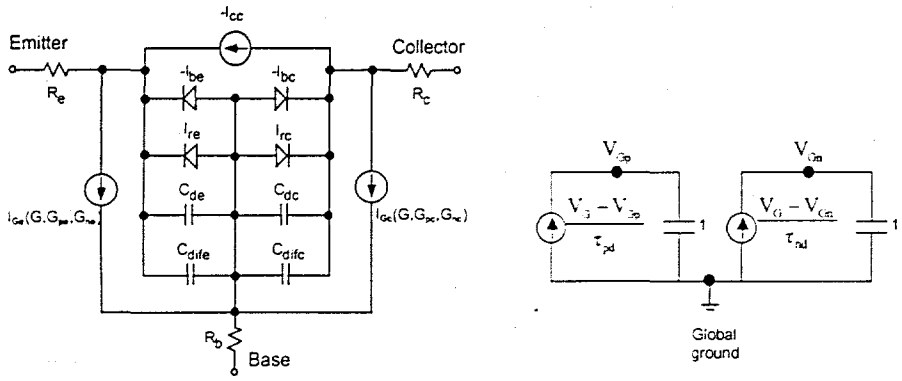

Fig. 1. Basic Gummel-Poon BJT model including photocurrent sources I_{Ge} and I_{Gc}, corresponding to the emitter base and collector-base junctions, respectively. The temporal evolution of I_{Ge} and I_{Gc} is included through the dynamic quantities $G \equiv kV_G$, $G_{pe} \equiv kV_{Gpe}$, $G_{ne} \equiv kV_{Gne}$, etc. defined by delay subcircuits such as the one to the right for a *p-n* junction. G is the actual e-h generation rate and the G_{xy} are effective generation rates corresponding to the momentary value of the excess minority carrier charge in the collection volume of the various quasi-neutral regions. V_{Gxy} are fictitious voltages corresponding to the various generation rates, suitably scaled to be within a normal range for circuit simulation. The time constants τ_{xd} are dynamic delay times associated with the excess minority carriers.

depletion region. The first term gives rise to a "prompt" current density $J_{depi} = qGW_{dep}$, where W_{dep} of the width of depletion region. This current responds with a time constant given by the transport time $\tau_{dep} = W_{dep}/v$ across the depletion region, where v is the carrier drift velocity.

The photocurrent in the q-n regions adjacent to the depletion region is governed by the ambipolar transport equation. At low radiation dose-rates (low-injection), the ambipolar transport parameters become independent of dose-rate. This is also the case in the higher dose-rate regime where the SRH traps are saturated.[5-8] Hence, in both these regimes, the stationary ambipolar diffusion equation can be solved analytically and the following total photocurrent is derived for a *p-n* junction with cross section A:

$$I_G = qAG\left(W_{dep} + L_{pd} + L_{nd}\right) \quad \text{where} \quad L_{pd} = L_{ap}\tanh\left(W_n/2L_{ap}\right), \quad L_{nd} = L_{an}\tanh\left(W_p/2L_{an}\right) \tag{1}$$

Here, G is the stationary e-h generation rate, and L_{pd} and L_{nd} are effective diffusion lengths. W_n and W_p are the lengths and L_{ap} and L_{an} are the minority carrier diffusion lengths of the *n*-type and *p*-type q-n region, respectively. Corresponding expressions for the effective diffusion lengths in Hi-Lo regions have also been derived.[10]

A careful analysis shows that of Eq. (1) can be generalized to cover all dose-rate regimes from low-injection to the Auger regime using suitable unified expressions for L_{ap} and L_{an} or, alternatively, for the minority carrier lifetimes and diffusion constants versus dose-rate, as shown in the example of Fig. 2.[10]

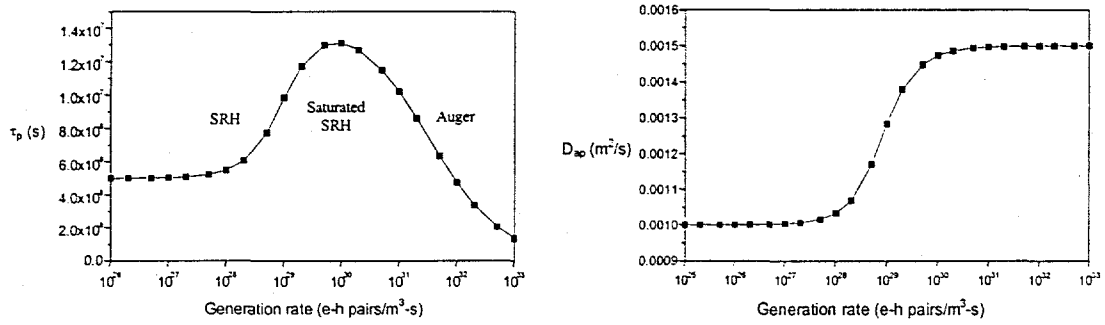

a) b)

Fig. 2. Examples of unified lifetime τ_p (a) and ambipolar diffusion coefficient D_{ap} (b) versus e-h generation rate G for *n*-type silicon with a doping density of 10^{22} m^{-3}. The generation rates shown can be converted to dose-rates (in rad/s) using $G/4.3\text{x}10^{19}$.

2.1. Dynamic model

To establish a dynamic electrical equivalent of the photocurrent effect for use in SPICE, we write the e-h generation rate as $G(t) = kV_G(t)$ where $V_G(t)$ is a fictitious time-dependent voltage and k is a suitable conversion factor. Any change in the generation rate will set up a transient build-up or discharge of minority carriers in the

quasi-neutral regions adjacent to the *p-n* junction. This represents a delay determined by the effective lifetimes τ_{pd} and τ_{nd} of the minority carriers in the *n*- and *p*-type regions, respectively, given by (see Eq. (1))[10]

$$\tau_{pd} = L_{pd}^2/D_{ap} = \tau_p \tanh^2(W_n/2L_{ap}), \qquad \tau_{nd} = L_{nd}^2/D_{an} = \tau_n \tanh^2(W_p/2L_{an}) \tag{2}$$

In the general case, the effective delay times change continually throughout the transient as a consequence of the dependence of the transport coefficients on the concentration of minority carriers within the collection volume.

In SPICE, the delay times may be represented in terms of the equivalent circuit shown in Fig. 1, which describes the temporal evolution of the total excess minority carrier charge in the q-n regions. In this model, the dynamic "voltages" V_{Gp} and V_{Gn} represent effective e-h generation rates G_n and G_p, which relate directly to the momentary value of the excess minority carrier charges within the collection volumes of the q-n regions. Hence, replacing G by G_n and G_p in the second and third terms, respectively, of the total stationary photocurrent in Eq. (1), we obtain the corresponding transient photocurrent given by:

$$I_G = qA\left[GW_{dep} + G_p L_{ap}\tanh(W_n/2L_{ap}) + G_n L_{an}\tanh(W_p/2L_{an})\right] \tag{3}$$

Also the ambipolar diffusion lengths L_{ap} and L_{an} are dynamic quantities that depend on G_p and G_n, respectively. SPICE determines simultaneously the "voltages" V_{Gp}, V_{Gn} and the delays τ_{pd}, τ_{nd} of the subcircuit in Fig. 1 by iteration at each time step of a transient analysis. The iteration starts from the values determined in the previous time step. At the first time step, the following initial values apply: $V_{Gp} = V_{Gn} = V_G(0)$, where $V_G(0) = G(0)/k$ corresponds to an initial steady state radiation intensity.

3. Simulation Examples

The above diode and BJT models were implemented in AIM-Spice,[10] and were tested for radiation pulses of 200 ns at different dose-rates and biasing conditions.

In the diode simulations, both n^+-p and n^--p-p^- diodes were investigated. Simulation results for the n^--p structure are shown as semilog plots in Figs. 3, to emphasize the time constants in the various regimes of the recovery phase of the diode. In these simulations, the bias voltage was 0 V and the series resistances in the diode and in the external circuit were taken to be zero.

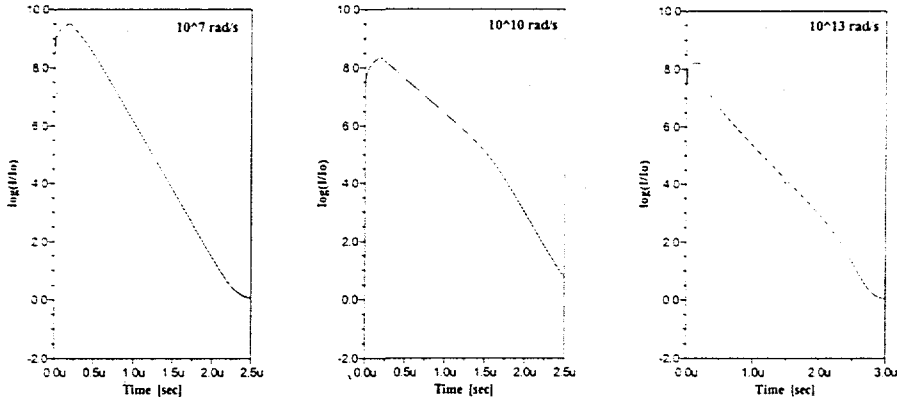

τ=1.3x10^{-8} s τ_1=2.6x10^{-8} s, τ_2=1.3x10^{-8} s τ_1=2.4x10^{-8} s, τ_2=1.4x10^{-8} s

Fig. 3. Photocurrent in n^+-p diode shown in a semilog scale. 200 ns radiation pulses at dose-rates of 10^7, 10^{10} and 10^{13} rad/s were applied. The time constants obtained from these plots are indicated below each figure.

We note that the overall recovery time increases with increasing dose-rate between 10^7 and 10^{10} rad/s owing to the saturation of the SRH traps. The two different time constants in the 10^{10} rad/s recovery correspond to the saturated SRH regime (2.6x10^{-8} s) and to the low-injection regime (1.3x10^{-8} s), the latter being in agreement with the time constant found in the 10^7 rad/s recovery. These values are also in agreement with the delay times calculated from Eq. (2). In a linear scale, the overall delay time at the dose rate of 10^{13} rad/s appears to be very much reduced compared to those of the lower dose-rates. This is caused by the initial dominance of rapid Auger recombination. However, the semilog plot reveals that the recovery enters the saturated SRH and the low-injection regimes with the same characteristic time constants as before. As expected, for the n^--p-p^-diode, significant reduced time constants were observed at all dose rates. These results indicate how primary SPICE parameters can be extracted from experiments.

In BJTs, the radiation induced photocurrent contributions can essentially be identified with those of the *p-n* junctions discussed above. However, an increase of majority carriers in the base, both from e-h production within the base and from injection from the neighboring regions, will result in a secondary minority carrier injection from the emitter. This mechanism provides a large internal gain in the photocurrent contributing to the collector current (active forward mode).

To test the BJT model of Fig.1, we considered *n-p-n* transistors with and without a Hi-Lo junction in the collector. In the simulations, a base-emitter voltage of 1 V and a collector-base voltage of 4 V were assumed. Both the base and the collector series resistances were varied. Examples of simulation results for the BJT structure with a Hi-Lo collector are shown in Fig. 4. The radiation dose-rate, the applied voltages, the series resistances and the type of current are indicated for each simulation. As for the diode simulations, we observe a set of time constants, which for the BJTs mainly can be identified with the delay times in the collector. These delay times reflect the various injection regimes (low-injection, saturated SRH and Auger) of the collector. In the low-injection regime, clearly observed in all the recoveries, we find time constants of about 3.5×10^{-8} s. For the BJT without a Hi-Lo collector, the corresponding time constant was almost an order of magnitude larger, which clearly demonstrates the radiation hardening effect obtained by using a Hi-Lo collector.

We also note that longer initial time constants are observed in the base photocurrent recovery (see Fig. 4 for 10^{10} rad/s) when using biasing circuit with finite resistance. This effect is presumably associated with a large secondary photocurrent and the recombination of excess carriers in the base.

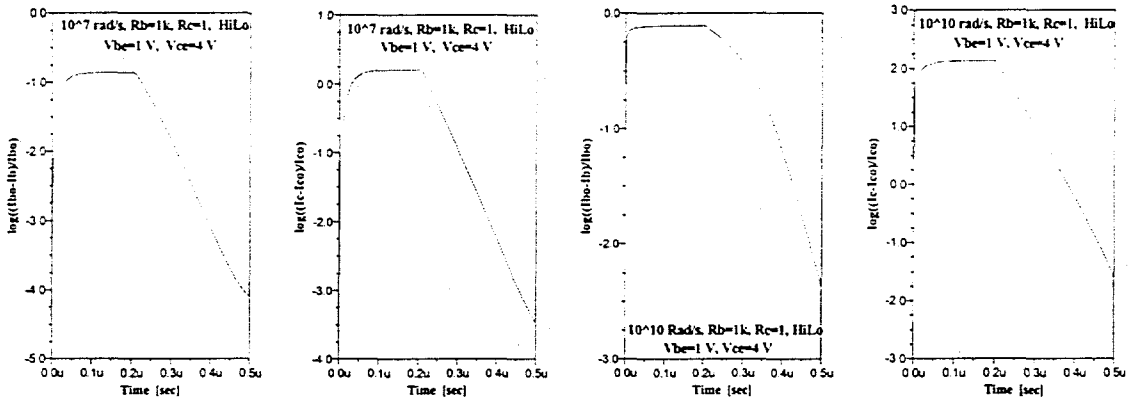

τ=0.036 μs τ=0.034 μs τ1=0.14 μs, τ2=0.037 μs τ=0.035 μs

Fig. 4. Base and collector photocurrents in an *n-p-n-n*$^+$ BJT (Hi-Lo collector) shown in a semilog scale. 200 ns pulses were applied at dose-rates of 10^7 (left) and 10^{10} (right) rad/s. The base and collector series resistances were R_b = 1k Ω and R_c = 1 Ω.

In conclusion, we have presented dynamic models for the photoelectric effect in *p-n* diodes and BJTs that are valid for a wide range of ionizing radiation dose-rates. The model has been implemented and tested in AIM-Spice.

References

[1] T. P. Ma and P. V. Dressendorfer, *Ionizing Radiation Effects in MOS Devices and Circuits*, John Wiley & Sons, New York, NY (1989). G. C. Messenger and M. S. Ash, *The Effects of Radiation on Electronic Systems*, Van Nostrand Rheinhold, New York, NY (1992).

[2] J. L. Wirth and S. C. Rogers, "Transient Radiation Current Generator Model for Semiconductor Devices", *IEEE Trans. Nuc. Sci.*, vol. 11, pp. 24-38 (1964).

[3] J. R. Florian, R. W. Jacobs, P. E. Micheletti, and E. E. King, "Improved Transient Response Modeling in IC's", *IEEE Trans. Nuc. Sci.*, vol. 31, no. 6, Dec. (1984). D. Long, J. Florian, and R. Casey, "Transient Response Model for Epitaxial Transistors", *IEEE Trans. Nuc. Sci.*, vol. 30, no. 6, pp. 4131- 4134 (1983).

[4] E. W. Enlow and D. R. Alexander, "Photocurrent Modeling of Modern Microcircuit p-n Junctions", *IEEE Trans. Nuc. Sci.*, vol. 34, no. 6, pp. 1467-1474 (1988).

[5] T. F. Wunsch and C. L. Axness, "Modeling of Time-Dependent Transient Radiation Response of Semiconductor Junctions", *IEEE Trans. Nuc. Sci.*, vol. 39, no. 6, Dec. (1992).

[6] A. N. Ishaque, J. W. Howard, M. Becker, and R. C. Block, "Photocurrent Modeling at High Dose Rates", *IEEE Trans. Nuc. Sci.*, vol.36, no.6, Dec. (1989).

[7] S. M. Sze, *Physics of Semiconductor Devices*. Second Edition, John Wiley & Sons, New York, NY (1981).

[8] T.A. Fjeldly, T. Ytterdal and M. Shur, *Introduction to Device Modeling and Circuit Simulation*, John Wiley & Sons, New York (1998).

[9] T.A. Fjeldly, Y. Deng and M. Shur, *Physics Based Modeling of High Intensity Ionizing Radiation Effects in Bipolar Junction Transistors*, unpublished (1999).

[10] AIM-Spice URL: http://www.aimspice.com. The present radiation model is not included in released version of AIM-Spice.

Sandia is a multiprogram laboratory operated by Sandia Corporation, a Lockheed Martin Company, for the United States Department of Energy under contract DE-AC04-94AL85000.